Check for updates

ChemPlusChem

Research Article
doi.org/10.1002/cplu.202300410

Chemistry Europe
European Chemical Societies Publishing

www.chempluschem.org

The Biomimetic Synthesis of Polyarylated Fluorenes, Relevant to Selaginellaceae Polyphenols, Leading to the Spontaneous Formation of Stable Radicals

Sundaravelu Nallappan,[a] Ringaile Lapinskaite,[a, b] Josef Hájíček,[a] Dominik Kunák,[a] Peter Čambal,[c] David Nečas,[a] Ivana Císařová,[d] Hazal Nazlıcan Atalay,[e] Tugba B. Tumer,[e] Ján Tarábek,[f] Karolina Schwarzová-Pecková,[c] and Lukas Rycek*[a]

This work reports a biomimetic synthesis of polyarylated fluorene derivatives. The molecules are formed *via* intramolecular electrophilic aromatic substitution, resembling a cyclization leading towards the natural selaginpulvilins from selaginellins. The scope of the reaction was investigated, and the products were obtained in 60–95% yields. Some of the compounds decompose to a stable radical. We investigated the nature and the origin of the radical using experimental methods, including EPR or electrochemical measurements, as well as theoretical methods, such as DFT calculations. Based on our observations, we hypothesize, that phenoxy radicals are formed in the first instance, which however undergo internal rearrangement to thermodynamically more stable carbon-centered radicals. The preliminary data also show the cytotoxic properties of some of the molecules.

Introduction

Plants from the genus *Selaginella* are living fossils, with an estimated age of 400 million years, which were used in folklore medicines throughout the world and their extracts showed a variety of biological effects.[1–4] They are a source of a plethora of structurally diverse natural products. Besides some alkaloids or flavonoids, which are however common for other species as well, a lot of attention was drawn to polyphenolic compounds, specific only for *Selaginella* plants.[5]

This Selaginellaceae polyphenol family includes, among others, selaginellins (**1**),[6] selaginpulvilins (**2**),[7,8] and recently isolated selagibenzophenones (**5**)[9–11] (Figure 1). The structural curiosity and the biological activity of these metabolites attracted the attention of synthetic as well as medicinal chemists. We reported a formal synthesis of selaginpulvilins C and D,[12] as well as selagibenzophenones A–C,[13,14] and clarified structural ambiguities, related to selagibenzophenone B. We also developed several derivatives of selagibenzophenone A (**5**) and identified a compound with selective cytotoxicity toward the prostate cancer cell lines, with negligible toxicity toward the healthy cells.[15] The biosynthesis of the Selaginellaceae polyphenols is believed to proceed *via* orsellinic acid derivative **4**, formed from polyketide **3**. Its further arylation furnishes the structural motif of selaginellins (**1**), which eventually undergo intramolecular Friedel-Crafts-like arylation to form the fluorene skeleton of selaginpulvilins (**2**, Figure 1). The experimental evaluation of the intramolecular cyclization was carried out by Yin, who demonstrated that the treatment of selaginellin A derivative with formic acid leads to the formation of selaginpulvilin A core.[8] The biogenesis of selagibenzophenones A and C is far less explored but presumably proceeds from orsellinic acid derivative **4** as well. Up to date, fluorene **7** or fluorenol **8**, which would result from an intramolecular cyclization of selagibenzophenone A (**5**) or related alcohol **6** (a possible biosynthetic precursor of **5**), has not been described (Figure 1, right-hand side).

In this contribution, we explore a chemical synthesis of the unnatural fluorene derivatives **7** and **8**, which are formed *via*

[a] Dr. S. Nallappan, Dr. R. Lapinskaite, Prof. J. Hájíček, D. Kunák, Dr. D. Nečas, Dr. L. Rycek
Department of Organic Chemistry, Faculty of Science
Charles University
Hlavova 8, 128 00 Prague (Czech Republic)
E-mail: rycekl@natur.cuni.cz

[b] Dr. R. Lapinskaite
Department of Organic Chemistry
Center for Physical Sciences and Technology Akademijos g. 7, Vilnius, 08412, Lithuania

[c] P. Čambal, Assoc. Prof. K. Schwarzová-Pecková
Department of Analytical Chemistry, Faculty of Science
Charles University
Hlavova 8, 128 00 Prague (Czech Republic)

[d] Dr. I. Císařová
Department of Inorganic Chemistry, Faculty of Science
Charles University
Hlavova 8, 128 00 Prague (Czech Republic)

[e] H. N. Atalay, Prof. T. B. Tumer
Department of Molecular Biology and Genetics
Faculty of Arts and Science, Canakkale Onsekiz Mart University
Canakkale, 17020 (Turkey)

[f] Dr. J. Tarábek
Institute of Organic Chemistry and Biochemistry
Academy of Science of the Czech Republic
Flemingovo nám. 2, 166 10 Prague (Czech Republic)

Supporting information for this article is available on the WWW under https://doi.org/10.1002/cplu.202300410

© 2023 The Authors. ChemPlusChem published by Wiley-VCH GmbH. This is an open access article under the terms of the Creative Commons Attribution License, which permits use, distribution and reproduction in any medium, provided the original work is properly cited.

© 2023 The Authors. ChemPlusChem published by Wiley-VCH GmbH

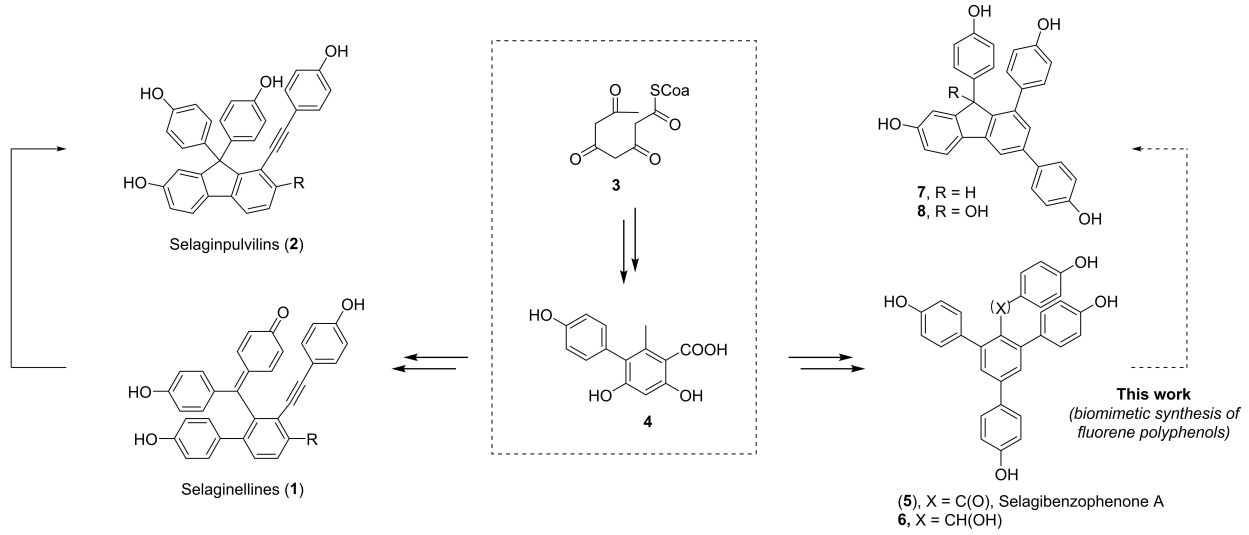

Figure 1. Structure and biogenesis of relevant natural products. On the left is depicted the conversion of selaginellins (**1**) to selaginpulvilins (**2**). On the right is depicted the structure of the natural product selagibenzophenone A and its chemical conversion to fluorenes, relevant to selaginpulvilins (**1**).

intramolecular Friedel-Crafts-like arylation, analogical to the one demonstrated for the biosynthesis of selaginpulvilins (**2**) from corresponding selaginellins (**1**). The Lewis acid-mediated cyclization proceeded smoothly to form the fluorene core **7**, but more demanding conditions were required for the Friedel-Crafts-like acylation to form the product **8**. The scope of the cyclization towards the various fluorenes and fluorenols was investigated and the reaction proved to be general for various substrates. For other methods of synthesis of the fluorene core, see the references.[16–19] We noticed an instability of some synthesized products which upon standing changed color to purple/red. Based on the combination of EPR spectroscopy, electrochemical methods, and density functional theory (DFT) calculation we propose the origin and the nature of the stable radical, which is a product of the partial decomposition of some of the synthesized compounds. The stable and persistent organic radicals[20] have attracted attention of the scientist for their potential application in the fields of electronics,[21] batteries,[22] or magnetic materials.[23] Moreover, preliminary data for compound **7a** revealed a moderate selective cytotoxic effect on colon cancer cell lines.

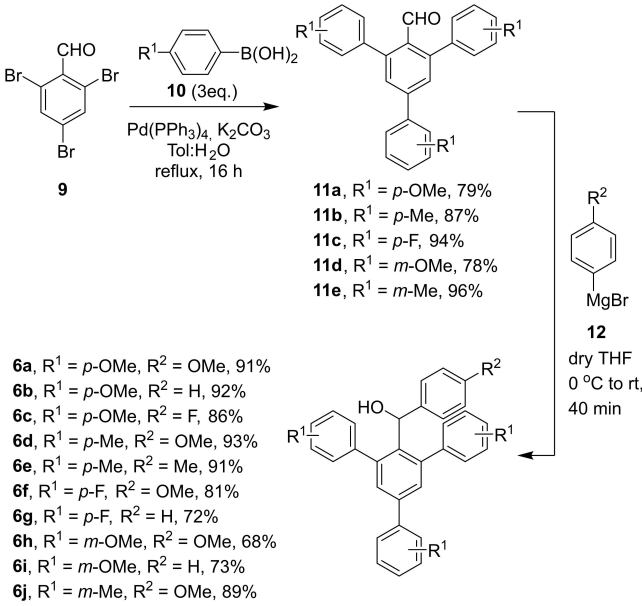

Scheme 1. Preparation of starting alcohols **6a**–**6j**.

Results and Discussion

Synthesis

The synthesis of the cyclization precursors **6a**–**j** is depicted in Scheme 1.

It commenced from 2,4,6-tribromobenzaldehyde (**9**), which was subjected to the Suzuki cross-coupling with three equivalents of boronic acids **10a**–**c**, yielding the desired arylated benzaldehydes in 79–94% yield. Further treatment of these aldehydes **11a**–**e** with various Grignard reagents **12**, resulted in the formation of secondary alcohols **6a**–**j** in 72–93% yield. These alcohols were further used for the boron tribromide-mediated cyclization.

The cyclization reactions of the secondary alcohols **6a**–**j** were carried out at room temperature. The amount of BBr_3 used depended on the number of methoxy groups present in the substrate. In total, we used 1.1 equivalent for each of the methoxy groups present and an additional 1.1 equivalent for the facilitation of the cyclization. First, the cyclization was carried out with the alcohols **6a**–**c** bearing methoxy groups in the *para* position of the rings C, D, and E (R^1 = *p*-OMe, Scheme 2). In the case of alcohol **6a**, bearing methoxy group in the *para* position of the ring A (R^2 = OMe), the corresponding fluorene **7a** was isolated in 85% yield. Fluorene **7b**, bearing no

© 2023 The Authors. ChemPlusChem published by Wiley-VCH GmbH

21926506, 0, Downloaded from https://chemistry-europe.onlinelibrary.wiley.com/doi/10.1002/cplu.202300410 by Canakkale Onsekiz Mart Uni, Wiley Online Library on [22/01/2024]. See the Terms and Conditions (https://onlinelibrary.wiley.com/terms-and-conditions) on Wiley Online Library for rules of use; OA articles are governed by the applicable Creative Commons License

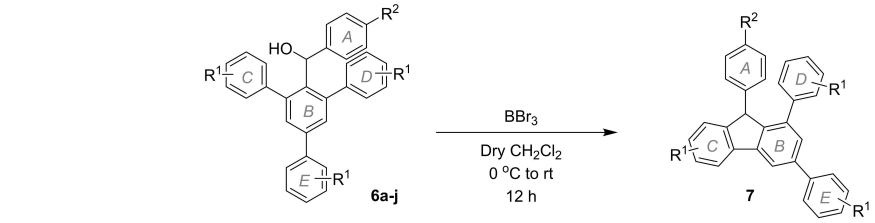

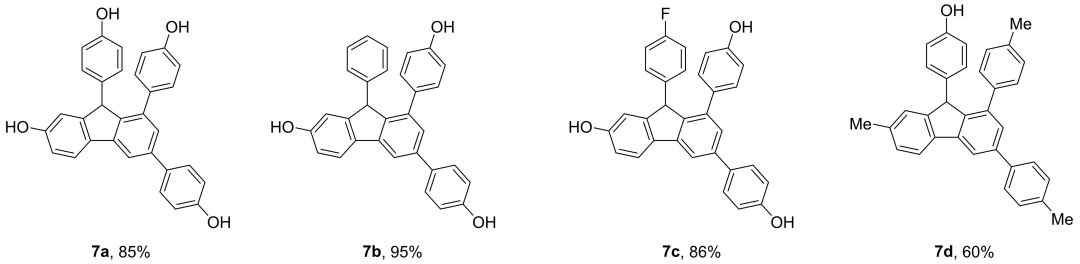

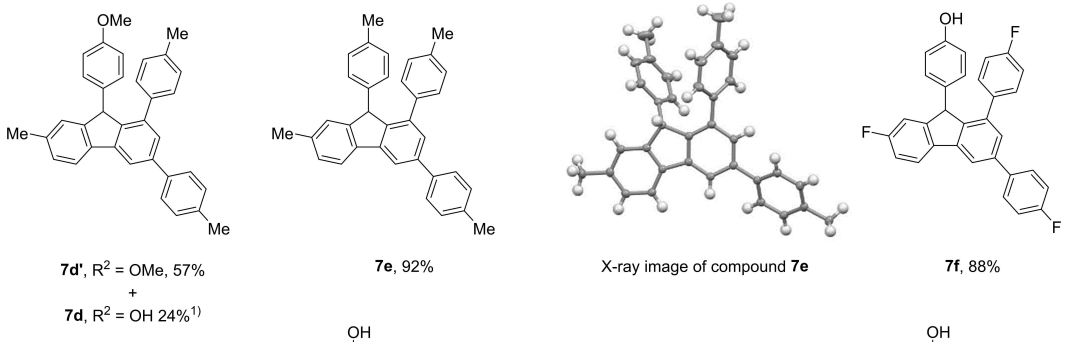

[1] 1.1 eqivalent of BBr_3 used

Scheme 2. Scope of the cyclization of secondary alcohols **6a**–**j** to fluorenes **7a**–**j** and view on molecule **7e**, displaying *R* configuration on chiral carbon C-9 (racemic crystal).

substitution at the ring A (R^2 = H) was isolated in excellent 95%. To investigate the effect of the electron-withdrawing (EWG) substitution, the cyclization was carried out with alcohol **6c**, bearing fluorine in the *para* position (R^2 = *p*-F). Corresponding fluorinated fluorene **7c** was obtained in 86% yield.

Next, we investigated the cyclization of alcohols **6d** and **6e** having methyl groups in the *para* position of the rings C, D, and E (R^1 = *p*-Me). When the reaction was carried out with alcohol **6d**, fluorene **7d** was obtained in 60% yield. The reaction was carried out in the presence of 2.2 equivalents of BBr_3. If the reaction was carried out in the presence of only 1.1 equivalent of BBr_3, the reaction provided 57% of the fluorene **7d'**, with the methoxy group still present in the molecule, and in addition, 24% of the demethylated **7d** was isolated as well. This suggests that cyclization happens fast and before demethylation. Cyclization of the alcohol precursor **6e**, bearing all methyl substituents (R^1 = R^2 = Me) led to the formation of the fluorene **7e** in an excellent 92% yield. The structure of fluorene **7e** was confirmed by X-Ray diffractometry. The suitable single crystal was obtained by evaporation of the $CDCl_3$ from the NMR sample of **7e**. Next, the alcohols with electron-deficient rings C, D, and E (R^1 = F) were evaluated.

The cyclization of alcohol **6f** with R^2 = OMe provided 88% yield of the desired fluorene **7f** and the cyclization of alcohol

© 2023 The Authors. ChemPlusChem published by Wiley-VCH GmbH

21926506, 0, Downloaded from https://chemistry-europe.onlinelibrary.wiley.com/doi/10.1002/cplu.202300410 by Canakkale Onsekiz Mart Uni, Wiley Online Library on [22/01/2024]. See the Terms and Conditions (https://onlinelibrary.wiley.com/terms-and-conditions) on Wiley Online Library for rules of use; OA articles are governed by the applicable Creative Commons License

6g without any substituent at the ring A (R^2 = H) proceeded in 76% yield. We then turned our attention to the alcohols with a *meta* substitution on the rings C, D, and E (**6h**–**j**). In such an arrangement, two possible regioisomers can be formed, where the ring C can be substituted either in position C-1 or C-3, depending on from which carbon the cyclization happens. We observed the preferential formation of C-3 substituted isomers in all the cases. In such a case the cyclization proceeds from less sterically hindered carbon. The cyclization of the alcohol **6h** bearing *meta* methoxy derivatives at rings C, D, and E (R^1 = *m*-OMe) and *para* methoxy substitution of the ring A (R^2 = *p*-OMe) provided an inseparable mixture of isomers **7h** and **7h'** in the ratio **7h**:**7h'** = 19:81 in overall 83% yield. The mixture of isomers was obtained also in the case of cyclization of alcohol **6i** bearing *meta* methoxy derivatives at rings C, D, and E (R^1 = *m*-OMe) and no substitution in the *para* position of the ring A (R^2 = H). Two isomers were obtained in overall 78% in the ratio **7i** and **7i'** in the ratio **7i**:**7i'** = 28:72. Last but not least the cyclization was carried out with the alcohol **6j** with the *meta* methyl substituents at the rings C, D, and E (R^1 = *m*-Me) and *para* methoxy substitution of the ring A (R^2 = *p*-OMe). The cyclization provided a mixture of fluorenes **7j** and **7j'** in the ratio **7j**:**7j'** = 20:80 and in overall yield 92%.

Similar intramolecular cyclization was observed in the case of secondary alcohol **16** (Scheme 3). This alcohol was prepared in two steps from 2,4-dichlorobenzaldehyde (**13**) by Suzuki cross-coupling with 4-methoxyphenyl boronic acids to yield aldehyde **14** and the addition of 4-methoxyphenylmagnesium bromide (**15**). Such alcohol contains the framework of another representative of the selaginellacea polyphenols, namely selagibenzophenone C.[9,14] The treatment of alcohol **16** with an excess of boron tribromide provided corresponding arylated fluorene **17** in 70% yield.

Further, selected alcohols were oxidized to corresponding ketones, which were then subjected to the cyclization conditions (Scheme 4). We found out that ketone **5a**, which was obtained in 74% yield from alcohol **6a** underwent intramolecular electrophilic acylation to yield the fluorenol **8a**. However, compared to the cyclization from alcohol, the cyclization from the ketone required extended reaction time (72 hours compared to 12 hours) and it provided only 63% of the corresponding fluorenol **8a**. Moreover, the alcohol was prone to the elimination of the water, to yield the ketone **18** (in case the LC/MS analysis was carried out from a methanolic solution we also detected a methanolic adduct **19**, resulting from a conjugate addition of methanol to the eliminated product **18**). Other undefined decomposition products were detected as well. Reactions of ketones **5b** (R^2 = H) and **5c** (R^2 = F), which were obtained from alcohols **6b** and **6c** in 82% and 91% yield, respectively, led to the formation of desired fluorenols as well. The absence of the electron donating group at ring A resulted in the facilitation of the reaction, which was finished in both cases in 12 hours, providing fluorenols **8b** and **8c** in 92% and 86% yield, respectively. However, these compounds proved to be unstable as well, even though, the decomposition was not as pronounced as in the case of fluorenol **8a**. This might be due to the lack of the hydroxyl group at ring A, and the necessity of forming the quinoid

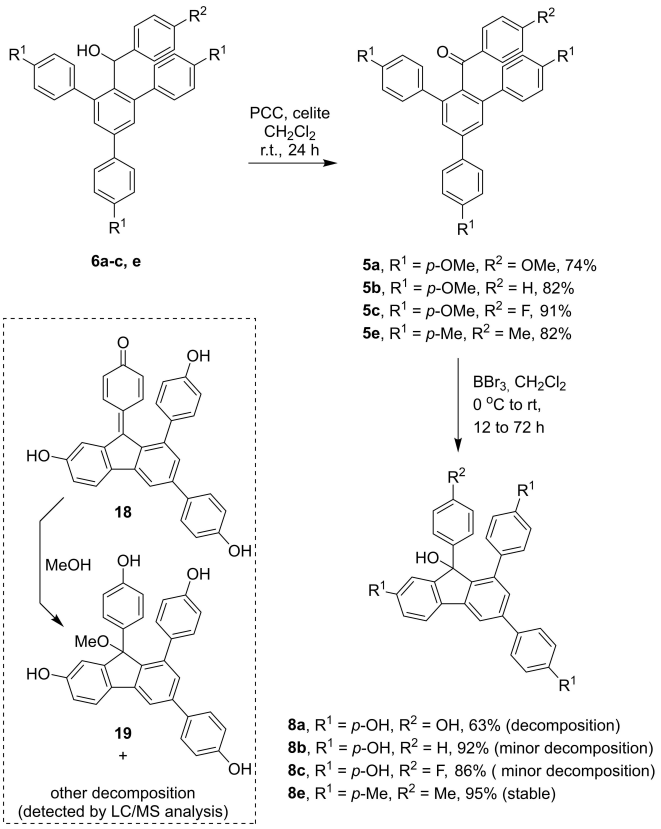

Scheme 4. Oxidation of alcohols **6a**–**c**,**e** to corresponding ketones **5a**–**c**,**e**, and their cyclization towards fluorenols **8a**–**c**,**e**. Decomposition of fluorenes containing phenolic moieties.

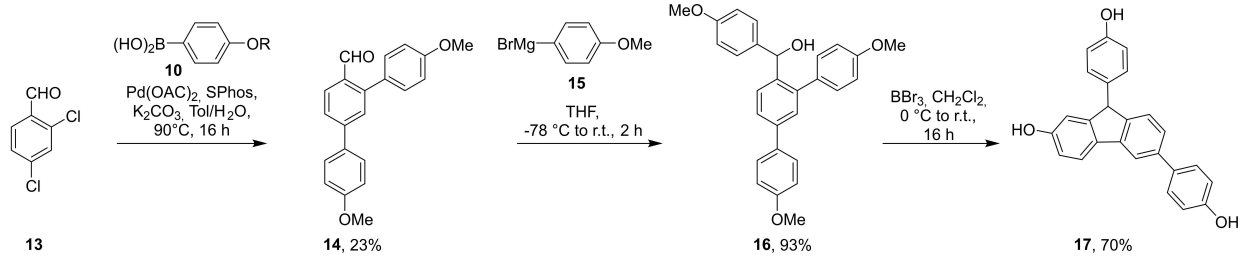

Scheme 3. Synthesis of secondary alcohol **16**, containing selagibenzophenone C framework and its cyclization towards corresponding fluorene **17**.

© 2023 The Authors. ChemPlusChem published by Wiley-VCH GmbH

21926506, 0, Downloaded from https://chemistry-europe.onlinelibrary.wiley.com/doi/10.1002/cplu.202300410 by Canakkale Onsekiz Mart Uni, Wiley Online Library on [22/01/2024]. See the Terms and Conditions (https://onlinelibrary.wiley.com/terms-and-conditions) on Wiley Online Library for rules of use; OA articles are governed by the applicable Creative Commons License

structure at rings D or E (1,6-elimination for **8a** vs. 1,8- or 1,10-elimination for **8b** and **8c**, see SI, Figure S17). The last cyclization was carried out from the cyclization of ketone **5e**, with *para* methyl groups at all the rings A, C, D, and E ($R^1 = R^2 =$ Me). Fluorenol **8e** was obtained in 95% yield. The absence of the phenolic OH group restricted the possibility of the elimination, and compound **8e** was, therefore, a stable compound, which did not undergo any further decomposition.

Decomposition to the stable radical

Some of the synthesized compounds, namely **7a, 7b, 7h, 17** (and to a lower extent also compounds **7c**, **7f, 7i**, and **7j**) changed color upon standing from colorless/white to red/dark-purple, or were directly obtained as such (noteworthy to say is that upon dissolving the sample in a solvent, e.g. methanol, resulted in the loss of the color, and its reappearing upon evaporation of the sample). Such a color change is a consequence of the partial decomposition of the synthesized products. The ^{1}H NMR analysis revealed a presence of unspecified signals in the aromatic region, belonging to the impurity. The most pronounced coloration was observed for compound **7a**; therefore, further discussion will relate mostly to it. The absence of the hydroxyl group in C-9 position in compound **7a** excludes the possibility of a simple elimination, observed for fluorenols **8a–c**. However, the LC/MS analysis of the methanolic solution of compound **7a** revealed a presence of the same methanolic adduct **19** (Figure 2, A), as detected in the case of analysis of fluorenol **8a**, discussed previously (see Scheme 4, for LC/MS spectra, see SI, Figure S1). This suggests, that some oxidative decomposition is taking place. Moreover, in the LC/MS spectra we also detected a compound with the mass corresponding to a peroxo adduct **20** (Figure 2, A). The MS analysis of fluorene **7b** (lacking the phenolic moiety on the ring A, $R^2 = H$). also clearly revealed a presence of methoxy and peroxo adducts. This prompted us to investigate if the oxidation proceeds in a sequence of single electron processes, and if some radicals are involved. Indeed, we detected an EPR signal in the spectra of a solid-state sample of **7a**. The spectrum was centered at g =2.0036, pointing to the presence of the organic radical with the g-factor close to that of the free electron. (Figure 2, B, and SI, Figure S2). The EPR signal was however lost upon dissolving the compound in methanol (see SI, Figure S2), correlating with the loss of color. This might be a consequence of a quenching of the solid-state stable radical in the solution. To explain the origin and the nature of the radical, the following considerations should be taken into account. The initial abstraction of the electron is most likely mediated by the molecular oxygen and happens from the lone pair of the phenol and it is accompanied by a loss of the proton, as known for phenols.[24] This could be confirmed by our observation made for fluorenes **7a**, **7d**, **7d'**, and **7e**. Out of these four compounds, the first two contain a free phenolic group and undergo oxidative decomposition, as could be noticed from ^{1}H NMR analysis (see NMR spectra in SI, Figure S61 and S67) and visually by their color change (more pronounced for compound **7a**). On the other hand, compounds **7d'** and **7e** which lack the free phenolic group did not change the color and no signs of decomposition were detected in ^{1}H NMR spectra.

The liability towards oxidation was further confirmed by electrochemical measurement. Cyclic voltammetry (CV) of **7a**, **7d**, **7d'**, and **7e** was performed on the boron-doped diamond electrode in acetonitrile (Figure 2C). The oxidation of **7a** is an irreversible process in agreement with the fact that all hydroxy groups are unpaired; *i.e.*, a quinone/hydroquinone-like system recognizable by the presence of a reversible peak pair on the CVs is not formed. There is an apparent gap between the oxidation potential of the first anodic peak of the phenol **7a** (+0.80 V) and **7d** (+1.20 V) reflecting the easier oxidation of **7a** with four phenolic groups in comparison with **7d** possessing one phenolic group. The initial step of electrochemical oxidation of phenolic compounds proceeds through a $1e^-/1H^+$ oxidation to a phenoxy-type radical,[25,26] which can be stabilized through resonance within the aromatic ring of the phenol moiety (see the resonance structures in SI, Figure S15). Further, a relatively large increase of the potential is for the oxidation of fluorene **7d'** (peak potential +1.45 V), containing methoxy, instead of the free phenolic group, underlying the importance of the free OH group. Worth attention is the possibility of the

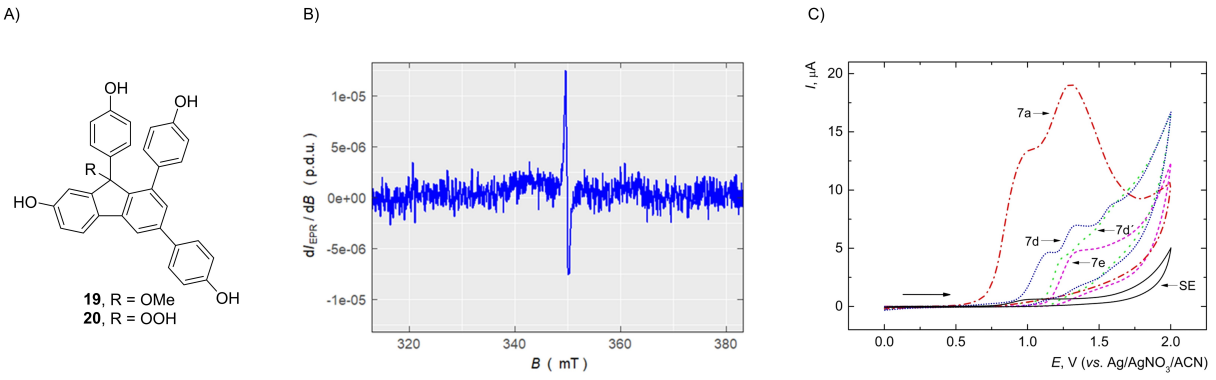

Figure 2. A) Decomposition of products of **7a** detected by LC/MS from methanolic solution. B) Representative EPR spectrum of the **7a** in powder form (m = 2.5 mg). C) Cyclic voltammograms of compounds **7a, 7d, 7d'**, and **7e** on the boron-doped diamond electrode in 1×10^{-2} mol dm^{-3} tetrabutylammonium perchlorate solution in acetonitrile as supporting electrolyte (SE). Scan rate 0.1 V s^{-1}, the concentration of the compounds 1×10^{-4} mol dm^{-3}.

© 2023 The Authors. ChemPlusChem published by Wiley-VCH GmbH

21926506, 0, Downloaded from https://chemistry-europe.onlinelibrary.wiley.com/doi/10.1002/cplu.202300410 by Canakkale Onsekiz Mart Uni, Wiley Online Library on [22/01/2024]. See the Terms and Conditions (https://onlinelibrary.wiley.com/terms-and-conditions) on Wiley Online Library for rules of use; OA articles are governed by the applicable Creative Commons License

electrochemical oxidation of compound **7e**, having only methyl substituents as aromatic hydrocarbon skeletons are usually redox-inactive.[27] The oxidation happened at the potential of +1.55 V, relatively close to that of **7d'**, It needs to be clarified, that the spontaneous oxidation is observed only for compounds **7a** and **7b**, while compounds **7d'** and **7e** undergo only electrochemical oxidation, while being air stable. This confirms two things, namely that the oxidation of the hydrocarbon core of the herein synthesized polyarylated fluorenes leads to relatively stable intermediates, and the presence of the free hydroxyl group (compared to e.g. methoxy or methyl groups) facilitates the oxidation significantly, allowing even for the spontaneous oxidation upon exposure to air. However, the observed unusual stability of the solid-state radical formed by the decomposition of **7a** can barely be explained by a simple extraction of the hydrogen atom and by the formation of the oxygen-centered phenoxy radical. Despite the fact, that persistent phenoxy radicals were described in the literature, usually, a kinetic stabilization through an adjacent bulky substitution is necessary. An example is a commercially available free galvinoxyl radical developed by Wiliams.[28] Such kinetic stabilization is missing in our case, and therefore, the chemical intuition governed us to "place" the radical at the C-9 position of the fluorene core (**S1**, Figure 3), where stabilization is ensured by an extended possibility of resonance. Moreover, several fluorene-based radicals were reported in the literature.[29,30] To support this, we conducted a series of density functional theory (DFT) calculations (see SI for details), which confirmed, that placing the radical at the C-9 carbon is energetically more beneficial than localizing it at any of the phenolic oxygens. If the radical is placed at C-9 carbon, the spin density distributes over rings A, B, and C. When the radical is placed at oxygen O-1 (**S2**), the Gibbs free energy difference increases by 3.5 kcal/mol, and the spin density is distributed only at rings C and B. Placing the radical at oxygen O-4 (**S3**), O-2 (**S4**), or O-3 (**S5**) results in the increase of Gibbs free energy by more than 5 kcal/mol (5.2, 5.4, and 5.5 kcal/mol, respectively). This correlates with the minimal level of the spin density distributions, which are located almost exclusively at the corresponding peripheral rings A, D, or E, with the minimal spin density distribution at any other ring of the fluorene core (Figure 3). Interestingly, if the spin distribution is localized at the fluorene core, it does not distribute at the peripheral rings D, and E and vice versa, despite the fact that one can draw corresponding resonance structures (see the resonance structures in SI, Figure S16). This is perhaps a consequence of the out-of-the-plane orientation of these rings. Moreover, while the spin densities of the phenoxy radicals **S5**, **S3**, **S2**, as well as **S4** are located at the peripheral phenol rings C, D, and E, well exposed to the environment the spin density in **S1** radical is located at less accessible positions, including C-9, C-1, or C-3 carbons, and thus a kinetic stabilization should be also considered, making the radical persistent. However, if the oxidation begins with the abstraction of the electron (and proton) from any of the phenolic groups, one cannot simply draw a resonance structure, where the radical is located at the C-9 carbon.

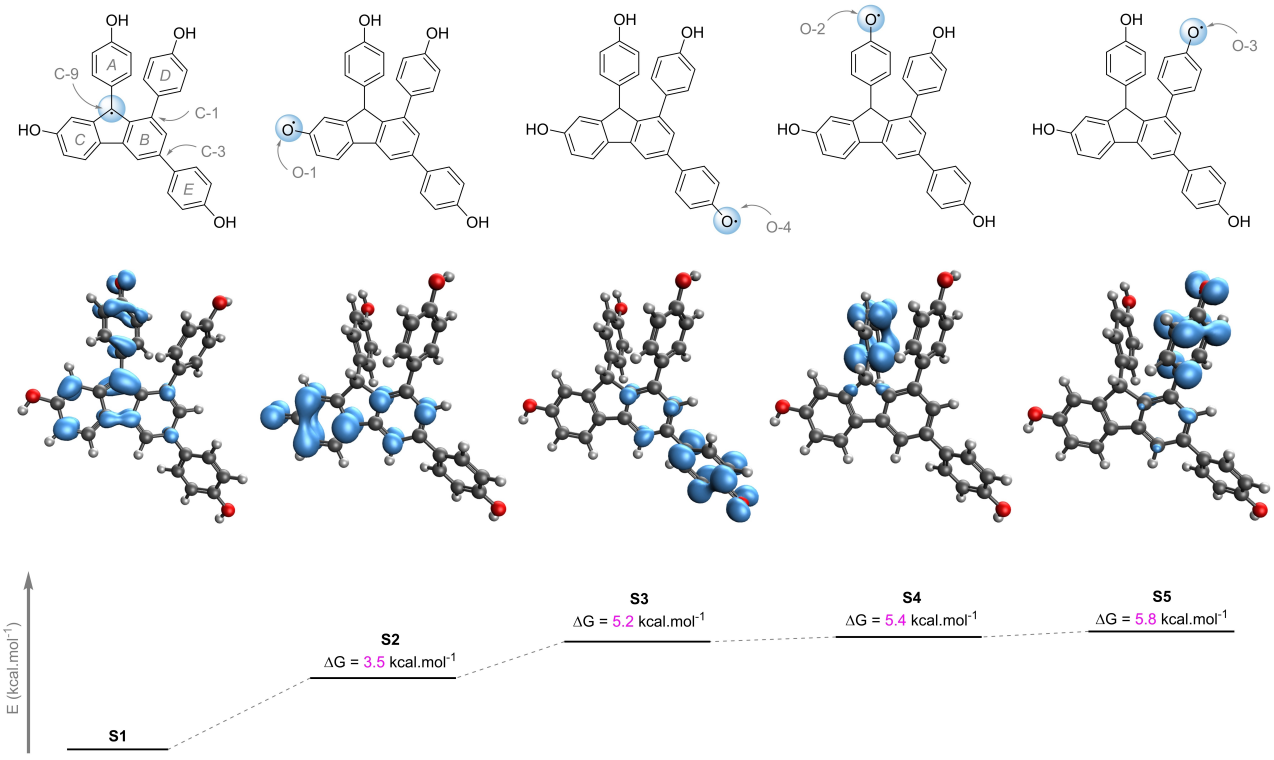

Figure 3. The possible radicals formed by oxidation of compound **7a**. Initial radical placements and corresponding spin density distributions for the calculated (uCAM–B3LYP/6-311 + G(d,p)) open-shell doublet models of **S1**–**S5** with relative Gibbs free energy differences. Surfaces were plotted at a 0.04 isovalue.

© 2023 The Authors. ChemPlusChem published by Wiley-VCH GmbH

21926506, 0, Downloaded from https://chemistry-europe.onlinelibrary.wiley.com/doi/10.1002/cplu.202300410 by Canakkale Onsekiz Mart Uni, Wiley Online Library on [22/01/2024]. See the Terms and Conditions (https://onlinelibrary.wiley.com/terms-and-conditions) on Wiley Online Library for rules of use; OA articles are governed by the applicable Creative Commons License

21926506, 0, Downloaded from https://chemistry-europe.onlinelibrary.wiley.com/doi/10.1002/cplu.202300410 by Canakkale Onsekiz Mart Uni, Wiley Online Library on [22/01/2024]. See the Terms and Conditions (https://onlinelibrary.wiley.com/terms-and-conditions) on Wiley Online Library for rules of use; OA articles are governed by the applicable Creative Commons License

Therefore, we propose the following mechanism of the formation of the stable radical derived from the phenol-containing fluorenes (Scheme 5). In the first step the oxygen-mediated abstraction of the electron, accompanied by the loss of the proton (mediated by the moisture) leads to the formation of the thermodynamically most stable phenoxy radical **S2**. We hypothesize, that the acidity of the fluorene hydrogen at C-9 might increase as a consequence of the presence of the radical. Such an acidity increase for protons next to radicals is documented in the literature.[31,32] The deprotonation of the C-9 carbon will result in the formation of the ketyl radical anion **S6**, in which the radical can be placed at C-9 carbon. The EPR signal, which we observe for the solid sample might therefore originate either from radical anion **S6** or its protonated version **S1**. The spin density distribution plot of **S6** shows a high degree of spin delocalization of the spin over the fluorene core and ring A. (Scheme 5, box). Similarly to **S1**, minimal spin density is found at the peripheral rings D and E. Interestingly, radical **S1** can be obtained by the same reaction mechanism even if the initial e^-/H^+ abstraction happens at any other phenolic oxygen (see SI, Figure S18).

Conclusions

We have developed a synthetic strategy towards polyarylated fluorenes, based on intramolecular electrophilic aromatic substitution. The cyclization proceeds easily from secondary alcohols, leading to fluorenes, or ketones, leading to fluorenols. The presence of a phenolic substitution at the certain position of the scaffold allows a decomposition of fluorenols to the corresponding quinoid structure *via* 1,6-elimination of water. Compounds which do not contain the phenolic substitution were stable. We also identified that the presence of a phenolic moiety in the fluorene molecules triggers an oxidative decomposition to form a radical, detectable in the solid state. We speculate, that the formation of the radical initiates by the extraction of the electron from the phenolic moiety, however, an internal rearrangement leads to a formation of a C-9-centered radical, which is thermodynamically stabilized by delocalization of the spin density. These suggestions are supported by electrochemical experiments, which underline the importance of the phenolic moieties, and DFT calculations, which demonstrate the delocalization of the spin density, and thermodynamic stabilization of the C-9 centered radical. Moreover, the kinetic stabilization by the phenol rings attached to the fluorene core should be considered as well.

The molecules **7a**, **8a**, and **17** are formed from precursors structurally related to naturally occurring selagibenzophenones A and C, *via* a mechanism described for the conversion of natural selaginellins (**1**) to selaginpulvilins (**2**). Therefore, the question arises, whether these compounds could as well be of a natural origin. In particular, the fact that isolated selagibenzophenone A (**5**) was described as a red compound, whereas selagibenzophenone A (**5**) synthesized by us previously is a white solid, makes us believe, that the coloration of the isolated sample can originate from trace impurities of fluorene **7a**, or fluorenol **8a**, respectively, by the colorful decomposition products thereof, which are described in this article. In addition, preliminary data show that compound **7a** possesses selective cytotoxic properties against colon cancer and prostate cancer cell lines with IC_{50} values of 24.0 and 38.7 μM, respectively, and low cytotoxicity towards healthy cell lines (IC_{50} = 100 μM) resulted in selectivity indexes of 4.2 and 2.6 for colon and prostate cancers, respectively. The above-mentioned results are a platform for further investigation of the compounds. In particular, compounds **7a**, **8a**, and **17** (together with their decomposition products, e.g. adducts **19** and **20**) can be used as standards in the search for compounds in natural sources. Moreover, the biological evaluation of the synthetic compounds

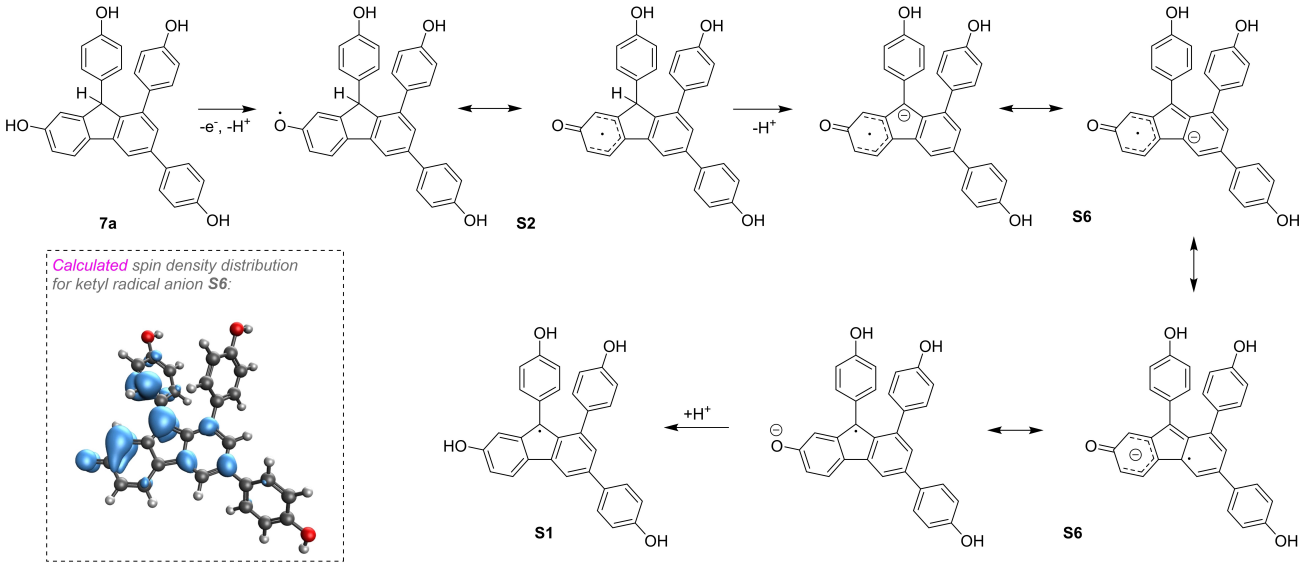

Scheme 5. Plausible mechanism of the formation of the stable radical from **7a** and calculated (uCAM-B3LYP/6-311 + G(d,p)) spin density distribution of the proposed ketyl radical anion **S6** with resonance structures depicting the formation of C-9 centered radical. The surface was plotted at a 0.04 isovalue.

© 2023 The Authors. ChemPlusChem published by Wiley-VCH GmbH

for their cytotoxic properties is currently ongoing, as well as the development of a stable radical for possible application is triggered.

Experimental section

All the chemicals were purchased from the common sources Sigma Aldrich, Acros Organics, Alfa Aesar, Strem Chemicals, PENTA Chemicals, Cambridge Isotope Laboratories, Inc. Unless otherwise noted, all of the materials are commercially available and used without further purifications or prepared by known methodologies. All the reactions were carried out in oven-dried reaction tubes. Reactions were monitored by thin-layer chromatography (TLC) using Merck silica gel 60 F254 precoated plates (0.25 mm) and visualized by UV fluorescence quenching using an appropriate mixture of ethyl acetate and hexanes. All the reactions were carried out on IKA magnetic stirrers. ^{1}H and ^{13}C NMR spectra were recorded on a Bruker 400 MHz (100 MHz for ^{13}C and 400 MHz for ^{1}H) instrument. ^{1}H NMR spectra were reported relative to residual $CDCl_3$ (δ 7.26 ppm) and DMSO-d_6 (δ 2.50 ppm). Whenever the residual peak is overlapping with the compound, spectra are reported as residual TMS. ^{13}C NMR was reported relative to $CDCl_3$ (δ 77.16 ppm) and DMSO-d_6 (δ 39.52 ppm). All chemical shifts δ are reported in ppm. Mass spectrometry was performed on a Thermo Fisher LTQ Orbitrap XL hybrid FT mass spectrometer with a combination of ion trap MS and the Orbitrap mass analyser. Infrared spectra were measured in KBr with a Thermo Nicolet AVATAR 370 FT-IR spectrometer. Unless otherwise stated, the reaction that requires heating was carried out with the oil bath as the heat source. Solvents used for extraction and column chromatography were laboratory grade and used after the distillation. All EPR experiments were performed on *Bruker* EMX^{plus} 10/12 CW (continuous wave) spectrometer equipped with the *Premium X* band microwave bridge. $g_{iso(center)}$ value of radicals was determined using a built-in spectrometer frequency counter and a ER-036TM NMR-Teslameter (*Bruker*). All $g-$Values were determined with the precision of $\pm$0.0002. The cyclic voltammetry (CV) experiments were performed on a μAutolab type III potentiostat equipped with the FRA module, controlled by the Nova 2.1.5 software (Metrohm Autolab, The Netherlands). Density functional theory (DFT) computations were carried out as unrestricted using the long-range corrected CAM–B3LYP[33] functional as implemented in Gaussian 16, revision C.01,[34] software. The triple-ζ quality basis set 6-311 + G(d,p) was applied to all atoms. The geometry-optimized open-shell doublet models of **S1**–**S5** and **22** were found as minima on the potential energy surfaces at the same level of theory. Spin density surfaces were visualized using IQmol software.[35] X-ray diffraction experiments for **7e** were performed on Bruker D8 VENTURE Kappa Duo PHOTONIII by IμS micro-focus sealed tube MoKα ($\lambda = 0.71073$) at temperature 120 K of measured crystals. The structures were solved by direct methods (XT)[36] and refined by full matrix least squares based on F^2 (SHELXL2018).[37] The hydrogen atoms on carbon were fixed into idealized positions (riding model) and assigned temperature factors either $H_{iso}(H) = 1.2\ U_{eq}$(pivot atom) or $H_{iso}(H) = 1.5\ U_{eq}$ (pivot atom) for methyl moiety. The hydrogen atoms on N and O were found on difference Fourier map and refined with assumptions of riding model. Crystallographic data are summarized in Table S1. X-ray crystallographic data have been deposited with the Cambridge Crystallographic Data Centre. Deposition Number 2284987 contains the supplementary crystallographic data for this paper. These data are provided free of charge by the joint Cambridge Crystallographic Data Centre and Fachinformationszentrum Karlsruhe Access.

The cytotoxic effects of the compound **7a** on PC-3 (human Caucasian prostate adenocarcinoma cells), HT-29 (human Caucasian colon adenocarcinoma cells), and HUVEC (human umbilical vein endothelial cells) cell lines, obtained from ATCC and cultured/maintained in DMEM (Gibco Life Technologies, Grand Island, NY) supplemented with 10% Fetal Bovine Serum (Gibco Life Technologies, Grand Island, NY), 100 U/mL penicillin-streptomycin were evaluated by the SRB (sulforhodamine B) assay as described previously.[15]

Supporting Information

Experimental procedures for the synthesis of the compounds together with spectral characterization, experimental procedures for EPR measurement, additional EPR data, DFT calculation details, and crystallographic details can be found in supporting information. The authors have cited additional references within the Supporting Information.[33–38]

Acknowledgements

The support of Specific University Research at Charles University, Charles University Research Centre UNCE, and Fond Junior (SVV 260690, UNCE/SCI/014, Fond Junior) is acknowledged. This study was partially funded by Çanakkale Onsekiz Mart University (Scientific Research Projects, ID: FIA-2021-3666 and FYL-2021-3564). We thank Dr. Martin Štícha for LC/MS measurement.

Conflict of Interests

The authors declare no conflict of interest.

Data Availability Statement

The data that support the findings of this study are available in the supplementary material of this article.

Keywords: selaginellacea polyphenols · biomimetic synthesis · radicals · spin density distribution · cytotoxicity

[1] J. A. Banks, *Annu. Rev. Plant Biol.* **2009**, *60*, 223–238.
[2] B. Křížkovská, R. Kumar, K. Řehořová, D. Sýkora, S. Dobiasová, D. Kučerová, M. C. Tan, V. Linis, G. Oyong, T. Ruml, J. Lipov, J. Viktorová, *Pharmaceuticals* **2021**, *14*, 16.
[3] M. Adnan, A. J. Siddiqui, A. Jamal, W. S. Hamadou, A. M. Awadelkareem, M. Sachidanandan, M. Patel, *Rec. Nat. Prod.* **2021**, *15*, 330–355.
[4] D. Yin, J. Li, X. Lei, Y. Liu, Z. Yang, K. Chen, *Evid.-Based Complement. Altern. Med.* **2014**, *2014*, 1–7.
[5] W. Li, G.-H. Tang, S. Yin, *Nat. Prod. Rep.* **2021**, *38*, 822–842.
[6] L.-P. Zhang, Y.-M. Liang, X.-C. Wei, D.-L. Cheng, *J. Org. Chem.* **2007**, *72*, 3921–3924.
[7] J.-S. Zhang, X. Liu, J. Weng, Y.-Q. Guo, Q.-J. Li, A. Ahmed, G.-H. Tang, S. Yin, *Org. Chem. Front.* **2017**, *4*, 170–177.
[8] X. Liu, H.-B. Luo, Y.-Y. Huang, J.-M. Bao, G.-H. Tang, Y.-Y. Chen, J. Wang, S. Yin, *Org. Lett.* **2014**, *16*, 282–285.

© 2023 The Authors. ChemPlusChem published by Wiley-VCH GmbH

21926506, 0, Downloaded from https://chemistry-europe.onlinelibrary.wiley.com/doi/10.1002/cplu.202300410 by Canakkale Onsekiz Mart Uni, Wiley Online Library on [22/01/2024]. See the Terms and Conditions (https://onlinelibrary.wiley.com/terms-and-conditions) on Wiley Online Library for rules of use; OA articles are governed by the applicable Creative Commons License

[9] W. Chen, Y. Peng, W. Huang, L. Zhou, X. Quan, Q. Zhao, D. Zhang, X. Sheng, Y. Luo, H. Zou, *Rec. Nat. Prod.* **2020**, *14*, 421–426.
[10] R. Liu, H. Zou, Z.-X. Zou, F. Cheng, X. Yu, P.-S. Xu, X.-M. Li, D. Li, K.-P. Xu, G.-S. Tan, *Nat. Prod. Res.* **2020**, *34*, 2709–2714.
[11] X. Liu, G.-H. Tang, H.-Z. Weng, J.-S. Zhang, Y.-K. Xu, S. Yin, *J. Asian Nat. Prod. Res.* **2018**, *20*, 1123–1128.
[12] L. Rycek, M. Mateus, N. Beytlerová, M. Kotora, *Org. Lett.* **2021**, *23*, 4511–4515.
[13] R. Lapinskaite, Š. Malatinec, M. Mateus, L. Rycek, *Catalysts* **2021**, *11*, 708.
[14] D. Kunák, M. Mateus, L. Rycek, *Eur. J. Org. Chem.* **2022**, *2022*, e202200014.
[15] R. Lapinskaite, H. N. Atalay, Š. Malatinec, S. Donmez, Z. O. Cinar, P. F. Schwarz, A. F. Perhal, I. Císařová, L. Labanauskas, T. M. Karpiński, V. M. Dirsch, T. B. Tumer, L. Rycek, *ChemistrySelect* **2023**, *8*, e202204816.
[16] For reviews on synthesis of fluorene cores see: a) R. P. Kaiser, I. Caivano, M. Kotora, *Tetrahedron* **2019**, *75*, 2981–2992; b) S. Patel, B. Rathod, S. Regu, S. Chak, A. Shard, *ChemistrySelect* **2020**, *5*, 10673–10691.
[17] For other Friedel-Crafts based fluorene synthesis see: a) G. Li, E. Wang, H. Chen, H. Li, Y. Liu, P. G. Wang, *Tetrahedron* **2008**, *64*, 9033–9043; b) S. Sarkar, S. Maiti, K. Bera, S. Jalal, U. Jana, *Tetrahedron Lett.* **2012**, *53*, 5544–5547; c) Q. Li, W. Xu, J. Hu, X. Chen, F. Zhang, H. Zheng, *RSC Adv.* **2014**, *4*, 27722-27725..
[18] For alternative polyarylated flurene core synthesis see: X–Ch Wang, R–L Yan, M–J Zhong, Y–M Liang, *J. Org. Chem.* **2012**, *77*, 2064-2068.
[19] For recent work related to fluorene synthesis see: a) L–Y Chen, J. Li, *J. Org. Chem.* **2023**, *88*, 10252-10256; b) Z. Jiang, K. Sekine, Y. Kuninobu, *Chem. Commun.* **2022**, *58*, 843-846; c) K. Dong, X. Fan, C. Pei, Y. Zheng, S. Chang, J. Cai, L. Qiu, Z.-X. Yu, X. Xu, *Nat. Commun.* **2020**, *11*, 2363.
[20] Z. X. Chen, Y. Li, F. Huang, *Chem* **2021**, *7*, 288–332.
[21] L. Ji, J. Shi, J. Wei, T. Yu, W. Huang, *Adv. Mater.* **2020**, *32*, 1908015.
[22] C. Friebe, U. S. Schubert, *Top. Curr. Chem. (Z)* **2017**, *375*, 19.
[23] I. Ratera, J. Veciana, *Chem. Soc. Rev.* **2012**, *41*, 303–349.
[24] M. Lj. Mihailović, Ž. Čeković, in *The Hydroxyl Group (1971)*, John Wiley & Sons, Ltd, **1971**, pp. 505–592.
[25] T. A. Enache, A. M. Oliveira-Brett, *J. Electroanal. Chem.* **2011**, *655*, 9–16.
[26] J. Vosáhlová, J. Sochr, S. Baluchová, Ľ. Švorc, A. Taylor, K. Schwarzová-Pecková, *Electroanalysis* **2020**, *32*, 2193–2204.
[27] Z. Senturk, *Curr. Drug Delivery* **2013**, *10*, 76–91.
[28] D. E. Williams, *Mol. Phys.* **1969**, *16*, 145–151.
[29] D. K. Frantz, J. J. Walish, T. M. Swager, *Org. Lett.* **2013**, *15*, 4782–4785.
[30] Y. Tian, K. Uchida, H. Kurata, Y. Hirao, T. Nishiuchi, T. Kubo, *J. Am. Chem. Soc.* **2014**, *136*, 12784–12793.
[31] J. C. Walton, *Chem. Soc. Rev.* **2021**, *50*, 7496–7512.
[32] J. C. Walton, *J. Phys. Chem. A* **2017**, *121*, 7761–7767.
[33] T. Yanai, D. P. Tew, N. C. Handy, *Chem. Phys. Lett.* **2004**, *393*, 51–57.
[34] "Citation | Gaussian.com," can be found under https://gaussian.com/citation/, **n.d**.
[35] "IQmol Molecular Viewer," can be found under http://www.iqmol.org/, **n.d**.
[36] G. M. Sheldrick, *Acta Crystallogr. Sect. A* **2015**, *71*, 3–8.
[37] G. M. Sheldrick, *Acta Crystallogr. Sect. C* **2015**, *71*, 3–8.
[38] S. P. Westrip, *J. Appl. Crystallogr.* **2010**, *43*, 920–925.

Manuscript received: July 31, 2023
Revised manuscript received: October 31, 2023
Accepted manuscript online: November 9, 2023
Version of record online: ■■, ■■

© 2023 The Authors. ChemPlusChem published by Wiley-VCH GmbH

21926506, 0, Downloaded from https://chemistry-europe.onlinelibrary.wiley.com/doi/10.1002/cplu.202300410 by Canakkale Onsekiz Mart Uni, Wiley Online Library on [22/01/2024]. See the Terms and Conditions (https://onlinelibrary.wiley.com/terms-and-conditions) on Wiley Online Library for rules of use; OA articles are governed by the applicable Creative Commons License

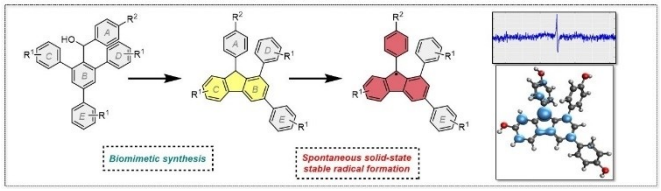

A biomimetic synthesis of polyarylated fluorenes similar to naturally occurring selaginpulvilines is reported in this work. Some of the synthesized fluorens spontaneously decompose to solid-state stable radical. Various techniques were employed, including cyclic voltammetry, EPR spectroscopy, and DFT calculation to shine a light on the origin and nature of the radical.

*Dr. S. Nallappan, Dr. R. Lapinskaite, Prof. J. Hájíček, D. Kunák, P. Čambal, Dr. D. Nečas, Dr. I. Císařová, H. N. Atalay, Prof. T. B. Tumer, Dr. J. Tarábek, Assoc. Prof. K. Schwarzová-Pecková, Dr. L. Rycek**

1 – 10

The Biomimetic Synthesis of Polyarylated Fluorenes, Relevant to Selaginellaceae Polyphenols, Leading to the Spontaneous Formation of Stable Radicals

21926506, 0, Downloaded from https://chemistry-europe.onlinelibrary.wiley.com/doi/10.1002/cplu.202300410 by Canakkale Onsekiz Mart Uni, Wiley Online Library on [22/01/2024]. See the Terms and Conditions (https://onlinelibrary.wiley.com/terms-and-conditions) on Wiley Online Library for rules of use; OA articles are governed by the applicable Creative Commons License